Free Energy Calculations of Ion Hydration: An Analysis of the Born Model in Terms of Microscopic Simulations

B. Jayaram,[†] Richard Fine,[‡] Kim Sharp,[†] and Barry Honig*,[†]

Department of Biochemistry and Molecular Biophysics, Columbia University, New York, New York 10032, and Department of Biological Sciences, Columbia University, New York, New York 10027
(Received: October 4, 1988)

The free energy perturbation technique is used in conjunction with Monte Carlo simulations to calculate the electrostatic contribution to the hydration free energy of a hypothetical cation whose charge varies in the range 0–3 au. The results are used to examine the validity of the continuum (Born) treatment of ion hydration. Saturation of the orientational polarizability of the water dipoles begins to become significant at values of the ionic charge of about +0.75, a considerably higher value than predicted from a Langevin analysis. Moreover, due to the opposing effect of electrostriction on the dielectric response, the continuum prediction of a quadratic charge dependence of the hydration free energy is reproduced for values of the ionic charge up to approximately +1.1. These results suggest that dielectric saturation is insignificant for monovalent cations. Above charges of 1.1 the first solvation shell becomes fully saturated while the remaining water molecules continue to respond quadratically with increasing charge. It is argued that to within a few percent the assumptions of the Born model (without corrections for dielectric saturation) can be justified in terms of microscopic simulations.

Introduction

An accurate theoretical treatment of the solvation of simple ions in water has been difficult to obtain despite the apparent simplicity of the system involved. One source of the difficulty arises from limitations in the understanding of the energetics, structure, and dielectric behavior of water molecules close to the ion. Given such complications, it is remarkable that treatments based on the Born model,[1,2] which assumes that the solvent is a dielectric continuum, are rather successful in reproducing the hydration enthalpies for a large number cations and anions of varying radii and charge.[3] The success of the Born model is particularly puzzling since the organization of water close to the ion, where ion–solvent interactions are the strongest, must be very different from that of bulk water.[4-7] In this study, a relationship between a microscopic description of water and continuum models is established by examining the dependence of hydration free energy on ionic charge. Changes in water structure around the ion as revealed by Monte Carlo simulations are correlated with the Born model through the continuum concepts of dielectric saturation and electrostriction.

The solvation free energy of an ion, ΔA, in the Born model, is a function of three variables, the charge of the ion q, the cavity radius a, and the dielectric constant ϵ of the solvent:

$$\Delta A = -q^2(1 - 1/\epsilon)/2a \qquad (1)$$

The expression is the sum of the electrostatic work done in discharging the ion in vacuum, and of charging the ion in a dielectric medium. (In an alternative and physically more meaningful formulation, eq 1 can be derived from the solvent reaction field induced by a point charge at the center of the ion.[8]) The only unknown in the Born formula is the radius, a, assigned to the ion.

Ionic radii defined from crystal structures are too small and consistently overestimate hydration free energies,[2] i.e., predict free energies that are too negative compared to experiment. However Latimer et al.[9] demonstrated some time ago that good agreement with experiment could be obtained for a number of ions if the radii used in the Born equation were chosen so as to account for the separation between the ion and the center of the water dipole. Hirata et al.[10] have recently argued (see also below) that this correction successfully incorporates the asymmetry of the water molecule into the continuum model. An alternative rationale for using larger radii has been based on electron density profiles in crystals, which indicate that covalent radii for cations and ionic radii for anions provide a meaningful and consistent basis for defining the cavity formed by an ion.[3] Calculated solvation enthalpies based on these radii (increased uniformly by 7%) are in excellent agreement with experiment even for multivalent ions. Independent of the physical interpretation associated with the use of different radii, it is remarkable that the Born model with little or no parametrization is capable of fitting a substantial number of data points.

Perhaps the greatest source of surprise is based on the fact that field strengths near an ion are on the order of 10^6 V/cm, which leads to the expectation that dielectric saturation will occur in regions of the solvent close to the ion.[11] The effect of dielectric saturation should be to lower the dielectric constant and hence to decrease calculated hydration energies. To account for the field dependence of the dielectric constant within the continuum scheme, the solvent around the ion has been treated either as concentric shells of different dielectric constant[12,13] or by varying the dielectric constant continually with distance from the ion based on a Langevin function description of solvent polarization.[14-18] However, the Langevin function neglects short-range correlations between solvent dipoles and is not appropriate for the description of the dielectric properties of associated solvents such as water.[19,20]

In an attempt to go beyond simple Langevin treatments, Booth[19] extended the dielectric theories of Kirkwood[21] and Frohlich[22] and found significant dielectric saturation effects at fields comparable in magnitude to those found near ions. However, this result is

[†] Department of Biochemistry and Molecular Biophysics.
[‡] Department of Biological Sciences.

(1) Born, M. *Z. Phys.* **1920**, *1*, 45.
(2) O'M Bockris, J.; Reddy, A. K. N. *Modern Electrochemistry*; Plenum: New York, 1970; Vol. 1, Chapter 2.
(3) Rashin, A. A.; Honig, B. *J. Phys. Chem.* **1985**, *89*, 5588.
(4) Mezei, M.; Beveridge, D. L. *J. Chem. Phys.* **1981**, *74*, 6902.
(5) Rao, M.; Berne, B. J. *J. Phys. Chem.* **1981**, *85*, 1498.
(6) Enderby, J. E.; Cummings, S.; Herdman, G. J.; Neilson, G. W.; Salmon, P. S.; Skipper, N. *J. Phys. Chem.* **1987**, *91*, 5851.
(7) Chandrasekhar, J.; Spellmeyer, D. C.; Jorgensen, W. L. *J. Am. Chem. Soc.* **1984**, *106*, 903.
(8) Gilson, M.; Honig, B. *Proteins* **1988**, *4*, 7.
(9) Latimer, W. M.; Pitzer, K. S.; Slansky, C. M. *J. Chem. Phys.* **1939**, *7*, 108.
(10) Hirata, F.; Redfern, P.; Levy, R. *Int. J. Quantum Chem.*, in press. Stokes, R. H. *J. Am. Chem. Soc.* **1964**, *86*, 979.
(11) Noyes, R. M. *J. Am. Chem. Soc.* **1962**, *84*, 513.
(12) Beveridge, D. L.; Schnuelle, G. W. *J. Phys. Chem.* **1975**, *79*, 2562.
(13) Abraham, M. H.; Liszy, J. *J. Chem. Soc., Faraday Trans. 1* **1978**, *74*, 1604.
(14) Millen, W. A.; Watts, D. W. *J. Am. Chem. Soc.* **1967**, *89*, 6051.
(15) Warshel, A.; Russell, S. *Q. Rev. Biophys.* **1984**, *17*, 283.
(16) Abe, T. *J. Phys. Chem.* **1986**, *90*, 713.
(17) Bucher, M.; Porter, T. L. *J. Phys. Chem.* **1986**, *90*, 3406.
(18) Ehrenson, S. *J. Phys. Chem.* **1987**, *91*, 1868.
(19) Booth, F. *J. Chem. Phys.* **1950**, *19*, 391, 1327, 1615.
(20) Schellman, J. A. *J. Chem. Phys.* **1957**, *26*, 1225.
(21) Kirkwood, J. G. *J. Chem. Phys.* **1939**, *7*, 911.
(22) Frohlich, H. *Trans. Faraday Soc.* **1948**, *44*, 238.

0022-3654/89/2093-4320$01.50/0

based on uncertain assumptions regarding water structure in the vicinity of ion.[20] Schellman[20] suggested that dielectric saturation may not be as important as is usually assumed, in part because electrostriction tends to increase the dielectric constant of the solvent in the vicinity of the ion, opposing the effect due to dielectric saturation. These issues are explored in this work via Monte Carlo simulations and free energy perturbation methods. An explicit molecular treatment of the solvent molecules provides a direct approach to the elucidation of the roles of dielectric saturation and electrostriction in the thermodynamics of ion hydration.

A considerable number of computer simulations of aqueous solutions of ions have been reported, many of which have focused on the structure of water around ions (see, for example, ref 4–7). Hydration enthalpies tend to be overestimated in such simulations, due in part to the neglect of three-body terms in the potential functions (see, e.g., ref 7). An effect of this neglect is the underestimation of water–water repulsions, primarily in the first shell of solvent molecules around the ion.

In this paper we present the results of a Monte Carlo based free energy simulation of ion solvation. We have focused, in particular, on the charge dependence of the solvation free energy. The Born model predicts that solvation energies vary as the square of the charge and experimental solvation energies do indeed exhibit a quadratic charge dependence.[3] For example, solvation energies of divalent and trivalent ions are approximately 4 and 9 times larger, respectively, than those of monovalent ions of similar radii. Our first goal has been to determine if simulations succeed in reproducing this quadratic charge dependence. Assuming that they do for the hypothetical cases of small charges (where saturation should not be a factor) our second goal has been to assess the effects of dielectric saturation for real ions. As discussed below, dielectric saturation is expected to produce a linear rather than quadratic dependence of hydration energy on charge, and this should be reflected in increasingly large deviations of any continuum prediction from experimental values as the magnitude of the charge increases. That such deviations are not evident (see, e.g., ref 3) suggests that the effects of dielectric saturation are not severe.

This suggestion is largely borne out by the results of this study. We find that for charges up to approximately +1, dielectric saturation is less of a problem than is generally believed, due in part, as anticipated by Schellman,[20] to the effects of electrostriction. At larger values of the charge, saturation in the first shell does become a factor but one that produces relatively small percentage effects. Our results do not point directly to a particular radius that might be appropriate for use in the Born model. On the other hand, the simulations do suggest that continuum models of ion hydration can be justified in terms of molecular simulations and hence that attempts to fit experimental data with simple physical parameters are not necessarily detached from "microscopic reality". This issue is considered in the Discussion.

Methods

To determine the difference in hydration free energy for two solutes i and j via perturbation simulations,[23-28] a coupling parameter, λ, is introduced into the potential function describing the solute–water interactions. The solute–water interaction energy for any value of the coupling parameter in the interval $|0,1|$ is evaluated as

$$E_\lambda = \lambda E_j + (1 - \lambda)E_i \qquad (2)$$

with $\lambda = 0$ referring to the solute i and $\lambda = 1$ to the solute j. A series of simulations are performed spanning successive ranges of λ in the interval 0–1, with a predefined $\Delta\lambda$ as the step size. In each simulation ensemble averages of $\exp[\{E(\lambda + \Delta\lambda) - E(\lambda)\}/kT]$ are formed with λ as the reference state. The relative free energies in each simulation are computed from

$$\Delta\Delta A(\Delta\lambda) = \Delta A(\lambda + \Delta\lambda) - \Delta A(\lambda) = (-1/kT) \ln \langle \exp[\{E(\lambda + \Delta\lambda) - E(\lambda)\}/kT] \rangle_\lambda \qquad (3)$$

where quantities enclosed by angular brackets refer to ensemble averages. The total free energy difference between states ($\lambda = 0$) and ($\lambda = 1$) is then

$$\Delta A_{ij} = \Delta A(\lambda{=}1) - \Delta A(\lambda{=}0) = \sum \Delta\Delta A(\Delta\lambda) \qquad (4)$$

The Monte Carlo simulation methodology used here is described elsewhere.[29] A modified Metropolis procedure[30] incorporating force bias[31] and preferential sampling[32] was used.

Monte Carlo computer simulations in the (T,V,N) ensemble at a temperature of 25 °C were performed to determine the free energy of hydration of an ion as a function of charge. The simulation system consisted of one cation and 215 water molecules at a density of 1 g/mL. These were enclosed in a box of half-edge-length 9.5 Å. The charge on the ion was varied from 0 to +3 au in 15 steps of 0.2 au. This charging procedure is the counterpart to the charging of an ion in a dielectric medium in the Born model. The midpoint of the charge range covered in each simulation is defined as the reference state. For instance, in a simulation varying the charge from 0 to 0.2 au, 0.1 au is defined as the reference state. Each simulation thus gives two values for relative free energies, i.e., one for 0.0–0.1 au and one for 0.1–0.2 au in the above example. Simple cubic periodic boundary conditions were used to approximate the macroscopic system. Solute–solute interactions were not considered. Thus the system studied corresponds to the solute at infinite dilution.

Ion–water interactions were computed with the potential function of Jorgensen and co-workers[7] under minimum image convention. The 6-12 parameters for the ion–water interactions were taken from ref 7 and correspond to those of a sodium ion in water. Water–water interactions were modeled by the TIP4P representation[33] with a spherical cutoff of 7.75 Å. The TIP4P model for water is reported to have a dielectric constant of about 50.[34] All ion–water interactions within a box were included. Thus, the cutoff for these interactions ranged from 9.5 Å for interactions along a line parallel to the edge of the box to 13.5 Å for interactions along the diagonal. The advantage of not using a spherical cutoff for ion–water interactions is that a larger number of terms are included if all waters in a box are allowed to interact with the ion. The disadvantage for the purposes of this study is that it is difficult to make a direct comparison to the Born model with a specific spherical cutoff radius. For the purposes of comparison, we have assumed that the effective cutoff radius in the simulations is 11 Å (the average of 9.5 and 13.5 Å). That is, the simulation results are compared to the Born prediction for a sphere of bulk solvent extending out to 11 Å. In addition we have used a Born "correction" that corresponds to the continuum contribution due to solvent molecules beyond a particular radius. For example, the results in Table I use a Born correction for ion–solvent interactions beyond 11 Å.

The initial configuration in each simulation was taken from a preequilibrated trial run on the ion–water system with appropriate charge on the ion. Each simulation involved a total of $\sim 3 \times 10^6$ configurations. Convergence is followed by monitoring the relative free energy. Representative convergence profiles of the calculated free energies are shown in Figure 1. Also shown in

(23) Mezei, M.; Beveridge, D. L. Free Energy Simulations. In *Computer Simulations and Biomolecular Systems*; Beveridge, D. L., Jorgensen, W. L., Eds.; Annals of the New York Academy of Sciences, No. 494, New York, 1986, and references therein.
(24) de Leeuw, S. W.; Perram, J. W.; Smith, E. R. *Ann. Rev. Phys. Chem.* **1986**, *37*, 245.
(25) Jorgensen, W. L.; Ravimohan, C. *J. Chem. Phys.* **1985**, *83*, 3050.
(26) Lybrand, T. P.; Ghosh, I.; McCammon, J. A. *J. Am. Chem. Soc.* **1985**, *107*, 7793.
(27) Bash, P.; Singh, U. C.; Langridge, R.; Kollman, P. *Science* **1987**, *236*, 564.
(28) Straatsma, T. P.; Berendsen, H. J. *J. Chem. Phys.*, in press.
(29) Jayaram, B. Ph.D. Thesis, City University of New York, 1987.
(30) Metropolis, N.; Rosenbluth, A. W.; Rosenbluth, M. N.; Teller, A. H.; Teller, E. *J. Chem. Phys.* **1953**, *21*, 1087.
(31) Rao, M.; Pangali, C.; Berne, B. J. *Mol. Phys.* **1979**, *37*, 1773.
(32) Owicki, J. C.; Scheraga, H. A. *Chem. Phys. Lett.* **1979**, *47*, 600.
(33) Jorgensen, W. L.; Chandrasekhar, J.; Madura, J. D.; Impey, R. W.; Klein, M. L. *J. Chem. Phys.* **1983**, *79*, 926.
(34) Neumann, M. *J. Chem. Phys.* **1986**, *85*, 1567.

TABLE I: Calculated Relative Free Energies of Hydration (kcal/mol)

free energy simulation					simulation energy with Born correction[a]	Born energy
q	$q + \Delta q$	$\Delta\Delta A$	$\pm 2\sigma$	ΔA		
0.0	0.1	−1.8	± 1.0	−1.8		
0.1	0.2	−4.3	± 0.3	−6.1		
0.2	0.3	−6.4	± 0.5	−12.5		
0.3	0.4	−8.2	± 0.5	−20.6		
0.4	0.5	−11.2	± 0.4	−31.9		
0.5	0.6	−13.3	± 0.4	−45.2		
0.6	0.7	−15.2	± 0.8	−60.4		
0.7	0.8	−17.3	± 0.2	−77.7		
0.8	0.9	−20.1	± 0.2	−97.8		
0.9	1.0	−22.0	± 0.5	−120	−135	−99
1.0	1.1	−24.4	± 0.6	−144		
1.1	1.2	−25.2	± 0.4	−169		
1.2	1.3	−26.3	± 0.5	−196		
1.3	1.4	−27.1	± 0.5	−223		
1.4	1.5	−28.5	± 0.1	−251		
1.5	1.6	−29.5	± 0.4	−281		
1.6	1.7	−31.3	± 0.2	−312		
1.7	1.8	−32.5	± 0.7	−344		
1.8	1.9	−32.7	± 0.4	−377		
1.9	2.0	−33.6	± 0.6	−411	−471	−400
2.0	2.1	−35.5	± 0.3	−446		
2.1	2.2	−36.3	± 0.7	−483		
2.2	2.3	−37.6	± 0.7	−520		
2.3	2.4	−38.7	± 0.4	−559		
2.4	2.5	−39.7	± 0.3	−599		
2.5	2.6	−40.4	± 0.4	−639		
2.6	2.7	−41.3	± 0.2	−680		
2.7	2.8	−42.4	± 0.8	−723		
2.8	2.9	−43.2	± 0.1	−766		
2.9	3.0	−44.3	± 0.5	−810	−945	−900

[a] ΔA + Born correction for ion–water interactions beyond 11 Å.

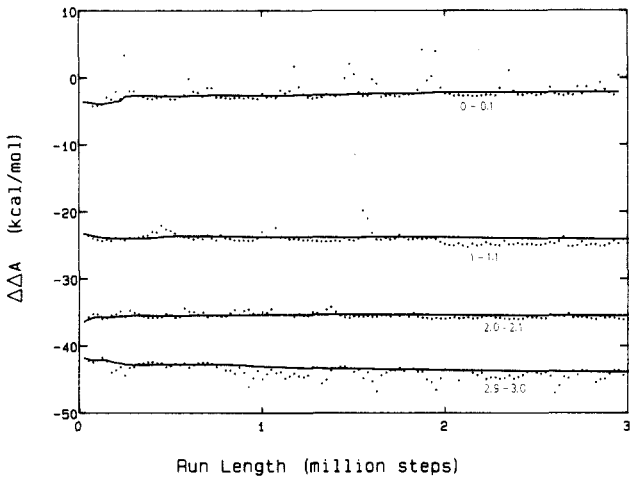

Figure 1. Convergence behavior of selected free energy simulations. Running mean free energy (solid line); successive block averages (dotted line). The charge ranges covered in the simulations are indicated on the figure.

the figure are the block averages taken over 25 000 Monte Carlo steps. Ensemble averages of the computed quantities are formed over the last 2×10^6 configurations of each run. The statistical uncertainties in the free energies are estimated by the method of batch means.[35] As a further check on the convergence of the calculated free energies and on the absence of hysteresis, some of the above simulations were repeated in the opposite direction (i.e., from λ to $\lambda - \Delta\lambda$) with random starting configurations. The relative free energies computed in both cases converged to within ±1 kcal/mol. For charges above +2.5 au on the ion, the estimated relative free energies converged slowly even though the runs were extended to 4×10^6 steps. Results are reported for relative free

(35) Erpenbeck, J. E.; Wood, W. W. *Modern Theoretical Chemistry*; Berne, B. J., Ed.; Plenum: New York, 1977; Vol. 6, Chapter 2.

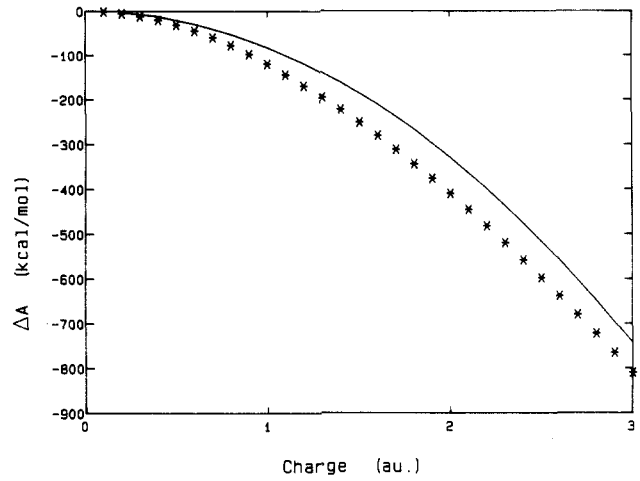

Figure 2. Calculated hydration free energies as a function of charge on the ion. Each point denoted by an asterisk refers to an individual free energy simulation. The solid line corresponds to the results of a Born model with a cavity radius of 1.68 Å truncated at 11 Å.

energies from 0 to 3 au, but discussion of results is confined mainly to the charge range of 0 to +2 au. In addition seven mean energy simulations were carried out with ion charges of 0, 0.25, 0.5, 0.75, 1.0, 1.5, and 2.0 au for structural analyses of the solvent. Calculations were carried out on either a Convex C1-XP computer or a Cray X-MP.

Results

The simulated relative free energies of hydration are shown in Table I along with statistical uncertainties at a 95% confidence limit. The solvation free energy given in Table I for a sodium ion is approximately −135 kcal/mol. This value is obtained from the calculated ΔA (−120 kcal/mol) with an added Born correction, defined above, which accounts for ion–solvent interactions beyond 11 Å. This is −15 kcal/mol for a monovalent ion, −60 kcal/mol for a divalent ion, and −135 kcal/mol for a trivalent ion.

As a test of the consistency of the simulations, it is of interest to compare the −135 kcal/mol hydration free energy of Na^+ given in Table I to the hydration enthalpy of −126 kcal/mol obtained by Jorgensen and co-workers[7] with the same potentials. Adding a Born correction of −22 kcal/mol to the latter value (based on the 7.5-Å spherical cutoff used in ref 7), an enthalpy of −148 kcal/mol is obtained. The room-temperature entropic contribution to sodium hydration is about +8 kcal/mol,[35] which, when subtracted from the hydration free energy reported in this work, predicts a hydration enthalpy of −143 kcal/mol. This value is in close agreement with the value of −148 kcal/mol we estimate from ref 7.

The free energies in Table I data are plotted in Figure 2 as a function of charge. The predictions of the Born model for a spherical shell extending out to 11 Å and a cavity radius of 1.68 Å are also plotted. This value for the cavity radius, which is used in ref 3, essentially reproduces the experimental hydration energy of Na^+. The Born curve in Figure 2 displays the quadratic charge response of a hypothetical ion with a radius of Na^+. It is evident from Figure 2 and from Table I that the simulations produce an approximately quadratic dependence of ΔA on charge for charges less than 1 au but that for larger values of q the behavior is no longer quadratic. A better description of the q dependence of ΔA can be obtained by plotting $\Delta\Delta A/\Delta q$ (i.e., the derivative of the hydration free energy) as a function of q as shown in Figure 3. The electrostatic component of $\Delta\Delta A/\Delta q$ is the mean reaction potential due to the water at the ion and should be linear in q if the Born model is obeyed (solid line in Figure 3). In contrast, the simulation plot has two linear portions, above and below an ion charge of +1.1 au. As is evident from the figure and from the correlation coefficients given in the figure caption, the simulations produce response curves that are linear to a remarkably high degree of precision.

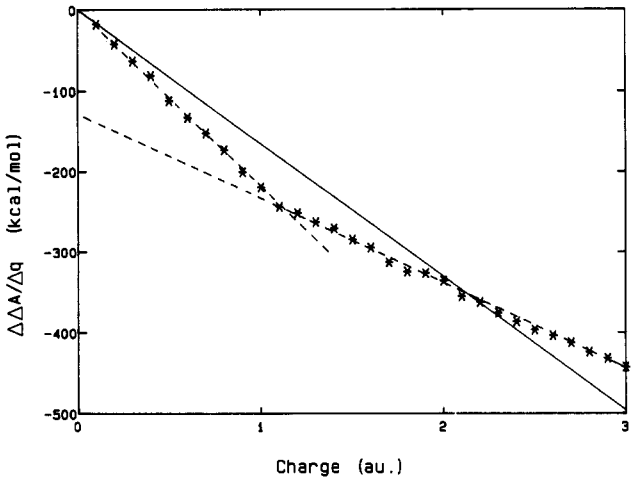

Figure 3. Calculated $\Delta\Delta A/\Delta q$ as a function of charge on the ion. Asterisks and the solid line are the same as for Figure 2. Dashed lines are least-squares fits to the simulation results. The line for values of q less than 1.1 has a slope of -225 ∓ 3, an intercept of 4 ∓ 2, and a correlation coefficient, r, of 0.999. The line for values of q greater than 1.1 has a slope of -107 ∓ 2, an intercept of -126 ∓ 3, and an r value of 0.995.

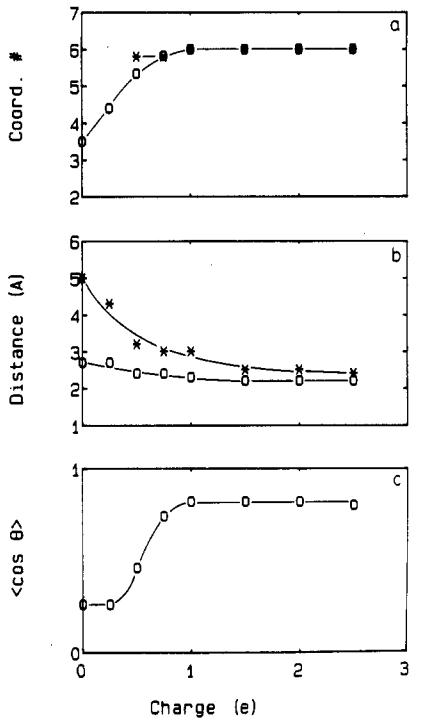

Figure 4. (a) Coordination number of first-shell waters: O, number of water molecules within a spherical shell of radius 3 Å around the ion; *, obtained from the integral of the first peak in the radial distribution function, $g(r)$. For the latter, the points for $q = 0$ and 0.25 are omitted due to the extremely broad first peak. (b) Distance to the first maximum (O) and minimum (*) in the ion–water (oxygen) radial distribution function. (c) Ensemble average of the radial orientation of water dipoles, $\langle\cos\theta\rangle$ in a spherical shell of 3 Å around the ion.

We first note that for values of q less than 1.1 the simulations reproduce the continuum prediction of a quadratic dependence of solvation free energy (linear dependence of the reaction potential) on ionic charge. To identify the factors that produce the abrupt change in slope at 1.1 au, a structural analysis of the water for several different values of q was undertaken. The results of this analysis for waters near the ion are shown in Figures 4 and 5. Briefly, as the charge on the ion increases, two types of structural changes in the waters near the ion are observed. The first is increased electrostriction, defined here as the tendency of waters to crowd closer to the ion as the ionic charge is increased. The second is increased orientational polarization, defined by the increase in the tendency of waters to align in the ionic electric

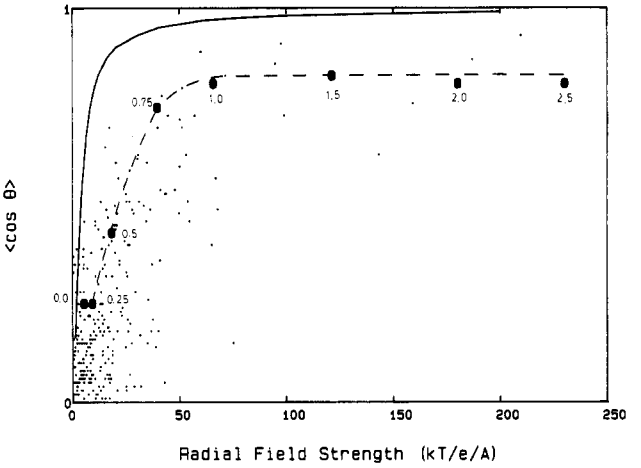

Figure 5. Radial orientation of water molecules as a function of radial field. Points correspond to molecules selected at random from random snapshots during the mean energy simulations plotted against the strength of the radial field calculated from the instantaneous positions of the ion and all other water molecules, excluding the selected molecule: O, ensemble-average values for the first-shell waters only, charge value indicated on the plot; dashed line drawn through these points; solid line obtained from the Langevin function.

field with increasing ionic charge. As illustrated Figures 4 and 5 and discussed below, both electrostriction and orientational polarization increase with increasing charge for ionic charges below 1 au. However, for ionic charges above 1 au, both effects plateau, leaving a completed first shell of six waters whose mean orientation is not affected by further increases in ionic charge.

The data on electrostriction are presented in Figure 4a,b. The solid line in Figure 4a shows the number of waters within a 3-Å shell of the ion (defined by the center-to-center distance from the ion to a water molecule) as a function of ionic charge. As the ionic charge increases from 0 to 1 au, the number of waters within 3 Å of the ion increases from 3.5 to 6. Beyond this charge there is no further increase. The same behavior is shown by the dashed line in Figure 4a, which represents the number of waters in the first shell of solvation defined by the integral of the first peak in the ion–water radial distribution function $g(r)$. Figure 4b shows the position of the first maximum and first minimum of $g(r)$ as a function of charge. These quantities traditionally define the center (median) and outermost extent of the first shell of solvation. These data clearly show shrinkage of the first shell as the ionic charge is increased from 0 to 1 au but negligible shrinkage for higher charge values. The convergence of these two lines also indicates the sharpening of the first peak of $g(r)$.

Figures 4c and 5 illustrate the tendency of waters to align in the electric field they see as the field is increased by increasing the ionic charge. In Figure 4c, this is shown by plotting the value of $\langle\cos\theta\rangle$ against ionic charge, where θ is defined as the angle between the dipole of the water molecule and a radius vector drawn from the ion to the center of that water molecule. The radial vector points in the direction of the applied electric field of the ion. The value of $\langle\cos\theta\rangle$ increases from 0.22 at zero charge (discussed below) to 0.82 at a charge of 1 au. However, the orientational polarization as measured by $\langle\cos\theta\rangle$ clearly saturates, remaining essentially constant at 0.82 as the ionic charge is further increased. Since a value of 1.0 would indicate perfect alignment of the dipoles in the field of the ion, this might be expected to be the saturation value. The fact that perfect alignment is not achieved can be attributed to interactions with second-shell waters that place constraints, due both to hydrogen bonding and dipole–dipole interactions, on the orientation of the first-shell waters.

Figure 5 contains a scatter plot of the radial orientation of water molecules selected at random from random snapshots during the mean energy simulations. The data are plotted against the strength of the radial field at the selected molecules calculated for that snapshot from the instantaneous positions of the ion and all other water molecules, excluding the selected molecule. This field thus

corresponds to the internal field acting on the water molecule in question. The ensemble average values of the orientation and radial field strength for solvent molecules in the first shell are also shown in Figure 5 and, again, clear saturation behavior is evident. $\langle \cos \theta \rangle$ begins to level off at an internal field value corresponding to a charge of about 0.75 au.

For nonassociated polar liquids without atomic polarization, the dependence of $\langle \cos \theta \rangle$ on internal field strength can be derived analytically and is described by a Langevin function. This function corresponds to the solid line in Figure 5. The shape of the dashed curve in Figure 5 resembles that of the Langevin function although it is clear that in the simulations, saturation sets in at higher field strengths and, as discussed above, the dipoles never become fully aligned along the radial direction. Figure 5 clearly illustrates that saturation of the orientational polarizability of the water dipoles is significantly overestimated by the Langevin analysis.

It appears curious that the plot of $\langle \cos \theta \rangle$ (Figure 4c) shows a residual alignment of water evident at zero ionic charge. This behavior is due primarily to statistical uncertainties when averaging over a small number of water molecules in the absence of an orienting force. In fact, the value of $\langle \cos \theta \rangle$ at zero charge is probably much closer to zero. At larger values of the charge where there is a strong orienting field, we have confirmed that $\langle \cos \theta \rangle$ reported in Figure 4 is a statistically "stable" value.

Discussion

The results presented in the previous section reveal a number of striking features of the response of TIP4P water to an increase in ionic charge. In agreement with the Born model, the derivative of the solvation free energy with respect to charge ($\partial \Delta A / \partial q$) is linear in charge (corresponding to a quadratic response in the solvation energy); however in contrast to the continuum prediction, there are two distinct ranges of a linear response (above and below a charge of 1.1 au) each with a different slope. Further, a more detailed look at the structure of the energetically important first-shell waters reveals a far more complex molecular response to increase in ionic charge than is suggested by a simple continuum model. In the Discussion we attempt to reconcile the continuum and microscopic descriptions of ion solvation. We first consider possible sources of error in the calculations and the impact they might have on the general conclusions that are reached.

Errors in Simulations of Ion Hydration. The principal sources of systematic error in the calculations are the absence of atomic polarization in the TIP4P water model, the use of cutoffs, and errors introduced by the periodic boundary conditions. The use of cutoffs, necessitated by the finite size of the simulation cell, will cause an underestimate of the solvation free energy since the interaction of the ion with water outside the cutoff radius, albeit weakly polarized, is neglected. In comparing to experiment, we have estimated the magnitude of the cutoff correction by assuming that water beyond the cutoff behaves as a bulk dielectric, i.e., according to the Born model. The magnitude of the relevant corrections are indicated in Table I and are discussed above.

A second problem arising from the finite size of the simulation cell is that periodic boundary conditions are applied at the cell boundary. This means that a water molecule at, say, the leftmost edge of the box, properly polarized to point toward the ion, will produce an image just outside of the rightmost edge of the box, improperly polarized to point away from the ion. Although the ion–water potential is truncated and hence the direct effect of this water will not be felt by the ion, the use of periodic boundary conditions will produce anticorrelated water dipoles at the walls of the simulation cell. Repulsive interactions between these dipoles will reduce the absolute magnitude of the calculated solvation energy.

Undoubtedly the most severe source of error in the simulations is that the ion–water potential functions are fit to properly account for gas-phase binding energies but the water–water potentials are not adjusted correspondingly to incorporate the increased dipole moment of waters that are strongly polarized by the ion. The absence of these three-body effects is a well-known problem and is the reason that most simulations systematically overestimate solvation energies. As discussed above, the calculations make an error of about 35 kcal/mol for the solvation energy of sodium. Since the effect of anticorrelated dipoles at the boundary is to decrease the solvation energy, the errors due to polarization alone are probably somewhat larger than 35 kcal/mol. The overestimation of the absolute values of solvation energy is a general property of all potential functions that do not account for polarization. In fact Straatsma and Berendsen[28] have recently reported free energy simulations of ion solvation using the SPC water model in which deviations from calculated and experimental values for sodium are about 30 kcal/mol once the Born correction (for solvent interactions beyond a cutoff radius of 9 Å) has been included.

The underestimate of water–water repulsion, primarily in the first shell, leads to the prediction that the simulations are overestimating the effects of dielectric saturation. This is because water–water interactions oppose the parallel alignment of dipoles; if this interaction is underestimated, the individual water dipoles will align more readily. Thus, the expectation is that saturation will set in above the value of $q = 1.1$ reported in this work. It should be pointed out in this regard that the sharp break observed in Figure 3 might be an artifact resulting from errors in the potential functions. However, the existence of a smooth transition between the two regions of linear dielectric response would not affect the basic conclusion that there are two distinct regions of linear response of the solvent molecules to increase in ionic charge.

Finally, it should be pointed out that the Born model accounts only for the electrostatic contribution to solvation, i.e., the Helmholtz free energy of solvent polarization, while the simulations account for both electrostatic and nonelectrostatic contributions to ion solvation. However, since the reference state of the simulations is the neutral ion, the energy of cavity formation contributes to the calculated change in free energy only if it changes with ion charge. This effect is small when compared to the large electrostatic contributions to ion solvation and has thus been ignored in the analysis.

Response of the First Shell. If dielectric saturation is introduced into the Born model, it has the effect of reducing the solvation free energies of ions relative to those anticipated by simple linear response theory. At the molecular level, a similar expectation arises: the principal dielectric response of a polar solvent to an increase in internal electric field is the energetically favorable orientation of the permanent dipoles in that field. If the dipoles are already fully oriented such that no further orientation can occur, the energetic response of the solvent is lowered relative to that expected without saturation. At the field strengths considered in this study, the effects of dielectric saturation are largely limited to the first shell.

Electrostriction, defined in the Results as the crowding of waters nearer the ion as the ionic charge is increased, has an effect that is opposite to that of dielectric saturation. As the number of water molecules in the first shell increases, the local dipole density increases, resulting in a more favorable interaction per unit volume with the ion. Further, as the first shell shrinks, the distance between the ion and the first-shell water dipoles decreases, resulting in more favorable interactions for each dipole. Both of these effects would tend to increase the dielectric response of the first-shell waters relative to, say, the predictions of a model that did not account for the effects of electrostriction.

Table II attempts to partition the dielectric response of the first shell into its individual contributions. (See Appendix A for a detailed definition of the terms that appear in the table). An estimate of the effect of shrinkage of the first shell can be made by calculating the change in potential at the ion due to the change in mean distance to the first-shell water dipoles (relative to the mean distance at zero charge) holding the number, N, of waters in the first shell fixed. The corresponding change in potential, $\Delta\phi_r$, is given in parentheses in the fifth row of Table II. The additional effect of increasing the number of waters in the first shell can be estimated by increasing the number of dipole–charge interactions contributing to the total sum from their original values at zero ionic charge to their final values at any given ionic charge.

TABLE II: Structural Parameters and the Effects of Electrostriction and Dielectric Saturation in the First Shell

	charge, au						
	0	0.25	0.5	0.75	1.0	1.5	2.0
R_{max}[a]	2.7	2.7	2.4	2.4	2.3	2.2	2.2
N	3.5	4.4	5.3	5.8	6	6	6
$\langle\cos\theta\rangle$	0.26	0.26	0.46	0.74	0.82	0.82	0.82
$\Delta\Delta A/\Delta q$[b]	0	−54	−112	−162	−220	−285	−336
$\Delta\phi'_{es}$[c]	na[e]	−20 (0)	−30 (−13)	−59 (−24)	−81 (−38)	−94 (−52)	−94 (−52)
$\Delta\phi'_{sat}$[d]	na	na	na	−7	31	153	256

[a] R_{max} is the distance in angstroms from the ion to the first water peak, N_c is the number of waters in spherical shell of 3 Å. [b] Values in kcal/(mol au) calculated from Table I. [c] Gain in negative potential due to electrostriction. Values in parentheses correspond to $\Delta\phi_r$. See Appendix A for details. [d] Loss of negative potential due to dielectric saturation. [e] Not applicable.

The two effects combine to give the total effect of electrostriction, $\Delta\phi_{es}$. Note that for a charge of 1 au, $\Delta\phi_{es}$ accounts for nearly half of the total potential but that this fraction decreases considerably for larger values of q.

An estimate of the potential difference, $\Delta\phi_{sat}$, due to the nonlinear response of $\langle\cos\theta\rangle$ with charge is made by comparing the calculated potentials to those predicted by a linear extrapolation of the potentials at low values of the electric field (see Appendix A). It is apparent that dielectric saturation has a smaller effect than electrostriction for values of q less than 1 au but that the relative contributions are reversed for larger values of q. While there is no way to completely separate the effects of saturation and electrostriction, the results do tend to confirm the conclusions drawn from Figures 4 and 5 that electrostriction is the major effect relative to simple linear response theory for $q < 1$ au, while dielectric saturation is the major effect for $q > 1$ au.

These findings are in sharp contradiction to the common view that dielectric saturation significantly lowers the effective dielectric constant of waters in the first shell, even around monovalent ions. A number of papers[16-18] have reported dielectric constants that are a function of distance from the ions and that approach the high-frequency value in the first shell. While Figures 4c and 5 do indicate the onset of saturation as measured by $\langle\cos\theta\rangle$ at values of q above 0.75, it occurs at a field that is much larger than predicted by a Langevin function (see Figure 5) thus demonstrating that previous treatments have overestimated the effects of saturation. Moreover, Figures 2 and 3 demonstrate that the first shell continues to behave as if it has a high dielectric constant, at least with regard to the free energy changes induced by an increase in charge, even beyond the point ($q = 0.75$) where the plot of $\langle\cos\theta\rangle$ has begun to level off. This is due to the fact that electrostriction continues to increase beyond this point (see Figures 4 and 5).

The results of the simulations thus strongly suggest that it is not appropriate to correct the Born model, at least for values of q less than 1 au, by lowering the effective dielectric constant in the vicinity of the ion. The effects of dielectric saturation on multivalent ions will be considered in the two following sections.

Two Regions of Linear Response. It is clear from the structural data we have presented that by a charge of 1 au, the first solvation shell of the ion is complete, with its librational dielectric degrees of freedom saturated at $\langle\cos\theta\rangle = 0.8$. Once the first shell has "exhausted" its ability to respond to an increase in field, it will exert a fixed potential at the position of the ion that will be independent of charge. Thus, the simplest interpretation of the two linear regions in Figure 3 is that the break corresponds to the value of q where the first solvation shell ceases to respond to increases in charge. This suggests a simple model for ion solvation for values of q above the break. The central ion appears to be surrounded by a fixed, frozen shell of six waters, with bulk water beyond the first shell. For such a model the water reaction potential, $\partial\Delta A/\partial q$, is given by

$$\partial\Delta A/\partial q = -N\mu\langle\cos\theta\rangle/R_m^2 + Cq \qquad (5)$$

where the first term gives the interaction of the N dipoles μ in the frozen shell with the ion, while the second term describes the response of all solvent molecules not in the first shell. R_m is the distance from the center of a frozen water dipole to the ion, and C is a constant. With values of 0.82 for $\langle\cos\theta\rangle$, $N = 6$, 2.18 D for μ, $\epsilon = 78.3$ for the bulk water, and the average distance to the first shell water dipole center for R_m of 2.75 Å (Table II), the first term gives −98 kcal/(mol au) as a constant contribution to $\partial\Delta A/\partial q$. Given the approximations involved (for example, treating the water as a point dipole), this value is in good agreement with the intercept of −126 ± 3 kcal/(mol au) obtained by fitting the curve above $q = 1$ au to a straight line and extrapolating this line back to $q = 0$.

The fact that the reaction potential of water beyond the first shell responds linearly with charge is not unexpected since even the first-shell waters respond linearly up to the break. If we assume that the Born model is valid for waters beyond the first shell, the constant in eq 5 should be given by

$$C = 332(1 - 1/80)(1/r_c - 1/11) \qquad (6)$$

where r_c is the effective radius of the cavity formed by ion and the first-shell waters and the 1/11 term again results from the use of 11 Å as an effective cutoff radius for ion–water interactions in the simulations. There is no obvious prescription for choosing a value for r_c, but the ~3.0-Å distance to the first minimum in $g(r)$ at $q = 1$ au provides a physically meaningful definition for the radius of the cavity formed by the first shell. This yields a slope of $C = -80$, which is in reasonable agreement with the slope of −107 kcal/(mol au) obtained for the line above $q = 1.1$ in Figure 3.

Modified Born Model with Dielectric Saturation. Due to the errors in the calculations discussed below, the numerical values of the free energies obtained in this work (and indeed in all simulations reported to date) are by no means accurate. Nevertheless, they do point to a simple physical model in which dielectric saturation in the first shell occurs fairly abruptly at some value of the ionic charge that is greater than 1 au and to solvent molecules beyond the first shell responding as a dielectric continuum. It should be emphasized that this picture is different than one that assumes that the first solvation layer is saturated for all values of the charge. The latter will necessarily underestimate the contribution of the first shell to the total solvation energy since it makes no allowance for the fact that for values of q less than some critical value q^*, which we find to be greater than 1, the effective dielectric constant is close to that of the bulk value.

It will prove useful in the discussion below to introduce a modified Born model that describes the qualitative behavior observed in Figure 3. If the Born model (eq 1) is extended to incorporate a shell of solvent, extending from the ionic cavity radius a to a radius b, which initially has a dielectric constant equal to the bulk, ϵ, and which saturates abruptly at a charge of q^* to yield a dielectric constant ϵ_1, then the solvation energy of the ion is given by (see Appendix B)

$$\Delta A = q^{*2}(1/\epsilon - 1)/2a \qquad q < q^* \qquad (7a)$$

$$\Delta A = q^{*2}(1/\epsilon - 1)/2a + q^*(q - q^*)(1/a - 1/b)(1/\epsilon - 1) + (q - q^*)^2(1/a - 1/b) \times (1/\epsilon_1 - 1)/2 + (q^2 - q^{*2})(1/\epsilon - 1)/2b \qquad q > q^* \qquad (7b)$$

The first term in eq 7b accounts for the Born-like response of the entire solvent to the charging process for charges less than q^*. The second term arises from the interaction of the inner solvent

shell reaction potential produced for q from 0 to q^* (where it exhibits the bulk dielectric behavior) with the charge above q^*. The third term arises from the additional reaction potential of the saturated inner shell interacting with charge above q^*. The fourth term describes the response of the solvent in the outer shell for charge greater than q^*. Note that the second term shows that even when the inner shell is "frozen" it still exerts a large q-independent field on the ion whose magnitude depends on the size of q^* and on the bulk dielectric constant. Thus this contribution to the interaction energy increases linearly with q even after saturation.

To estimate the effects of dielectric saturation on the predictions of the Born model, it is of interest to compare the predictions of eq 7 to those of eq 1. If we use a value of a 1.68 Å, which produces a solvation energy of Na^+ of about 99 kcal/mol (close to the experimental value), eq 1 would predict solvation energies for ions of the same radius of 396 and 891 kcal/mol for a divalent and trivalent cation, respectively. Deviations from these values obtained from eq 7 reflect the predicted effects of dielectric saturation. Assuming from the simulations that b = 3 Å and q^* = 1.1 au (as in Figure 3), it is still necessary to assign a value for the dielectric constant, ϵ_1, for the saturated shell of water. With a value of $\epsilon_1 = 2$ (which assumes that the only remaining dielectric response results from electronic polarizability) eq 7 predicts a solvation energy of 378 kcal/mol for the hypothetical divalent ion (5% deviation from eq 1) and 810 kcal/mol for the hypothetical trivalent ion (9% deviation from eq 1). These deviations would be about halved if the value of the high-frequency dielectric constant was about 4, as suggested by Hill.[36] If it were further assumed that due to the errors in the water–water potentials, dielectric saturation sets in at a value of $q^* = 1.5$ rather than 1.1, the deviations would be reduced by approximately another factor of 2.

The major conclusion from this simple numerical exercise is that the effect of dielectric saturation for multivalent ions is significant in terms of absolute energies but that the percent correction to the simple Born model is remarkably small. This would appear to explain, at least in part, why the Born model without accounting for saturation is capable of reproducing, within a few percent, the solvation energies of a large number of ions. The other reason is that even after the first shell has been saturated, it still exerts a large constant field on the ion. The first-shell ion–solvent interaction energy continues to increase linearly with q but with a large proportionality coefficient that is given by the magnitude of this field. Thus, the response in this region although no longer quadratic is still large. These results suggest that previous attempts to improve the Born model by incorporating saturation effects have significantly overestimated their importance. Equation 7 offers a possible route for improvement that is physically more reasonable, but, in our view, the magnitude of the corrections are not large enough to justify the use of an equation that lacks the elegant simplicity of the Born model and that contains additional parameters.

We thus conclude that the Born model, despite its shortcomings, is difficult to improve within a continuum treatment of the solvent. Given the inherent shortcomings of the model and the uncertainties in the choice of radii, the relative effect of dielectric saturation is not large enough to justify an explicit treatment.

Why the Born Model Works. For the Born model given in eq 1 to have any relationship to physical reality, a number of criteria have to be satisfied. First, for small values of q the solvation energy must increase quadratically with charge as predicted by a continuum model. This appears to be a general property of ions in dipolar solvents[37] and has been found to be the case in the simulations reported in this work. It has also been found[37] that in dipolar solvents the solvation free energy is approximately one-half the solute–solvent portion of the solvation energy. This result follows directly from continuum theory since for any linear dielectric the organization energy of the solvent is exactly one-half the solute–solvent interaction energy. It thus appears that even models that account for solvent structure reproduce the essential continuum behavior.

The second criterion for the success of eq 4 is that a single dielectric constant can be used to characterize the solvent. We have shown in this work that dielectric saturation is a relatively minor factor (at least in percent terms) for ions below a charge of 3, which leads to the prediction that it is reasonable to use the bulk dielectric constant for most ions (this may not be the case for small radii and large charges such as in the case of Be^{2+} where dielectric saturation may well be an important factor).

The final requirement is that it be possible to find an internally consistent set of radii that can be used in eq 1; that is, the Born model would be meaningless if the radius for each ion was used as a free parameter. Latimer, Pitzer, and Slansky[9] (LPS) obtained good agreement with experiment for monovalent ions by extending the crystallographic radii of cations by 0.85 and 0.1 Å for anions. Rashin and Honig[3] (RH) demonstrated that the covalent radii of cations and the ionic radii of anions (with a uniform 7% correction) also reproduced experimental data. Both models have some physical rationale. The adjusted LPS radius is a measure of the distance from the ion to the center of the water dipole, while the RH radii are related to size of the cavity formed by the ion, as defined by a region in space lacking solvent electron density. Thus, both models incorporate some information about the asymmetry of the water molecule, a point that has been emphasized recently by Hirata et al.[10] based on a study of ion solvation using the extended RISM integral equation theory.

It appears then that the underlying assumptions of the Born model can be justified in terms of microscopic simulations. Further simulations on ions of different radii and different charge may ultimately provide a clearer basis for the choice of radii that reproduce experimental quantities. On the other hand, it should be recalled that simulations using currently available potential functions make rather large errors in absolute solvation energies. In the meantime the Born model, though by no means exact, provides, with remarkable simplicity, an estimate of solvation enthalpies and free energies that are accurate to within a few percent. Recent extensions of the continuum model to the calculation of the solvation energies of nonspherical ions have yielded results of comparable accuracy.[8]

Acknowledgment. We gratefully acknowledge the stimulating and helpful discussions we have enjoyed with Professors P. J. Rossky and D. L. Beveridge. This work was supported by grants from the ONR (N00014-86-K-0483) and NIH (GM30518). Use of the Cray X-MP at the Pittsburgh Supercomputer Center was made possible through an NSF grant (DMB-8503489).

Appendix A: Equations Used To Estimate the Effects of Electrostriction and Dielectric Saturation in the First Solvent Shell

The main contribution to the reaction potential, $\Delta\phi_x$, comes from the dipole field of the first-shell waters. At any particular value of the ion charge, q, the potential from the first-shell waters is approximated by

$$\phi_f = N_q \mu \langle \cos\theta \rangle_q / R_q^2 \qquad \text{(A1)}$$

where N is the number of dipoles, μ is the dipole moment, $\langle \cos\theta \rangle$ is the mean radial orientation of the dipoles, and R is the mean distance of the dipoles from the ion. The subscript q refers to the mean values observed in the simulations at that value of q. For a given value of q, the gain in the reaction potential due to electrostriction can be partitioned into effects due to changes in R_q and to changes in N. The former, $\Delta\phi_r$, is given by

$$\Delta\phi_r = N\mu \langle \cos\theta \rangle_q (1/R_0^2 - 1/R_q^2) \qquad \text{(A2)}$$

where R_0 is the mean dipole distance at a charge of 0. The total change in potential due to electrostriction, $\Delta\phi_{es}$, accounts for the charge dependence of the number of dipoles in the first shell as well and is given by

(36) Hill, N.; Vaughan, W.; Price, A.; Davis M. *Dielectric Properties and Molecular Behavior*; Van Nostrand Reinhold: London, 1969; p 272.
(37) Yu, H.-A.; Karplus, M. *J. Chem. Phys.* **1988**, *89*, 2366.

$$\Delta\phi_{es} = \mu\langle\cos\theta\rangle_q(N_0/R_0^2 - N_q/R_q^2) \quad \text{(A3)}$$

where N_0 is the number of dipoles in the first shell at a charge of 0.

The loss in reaction potential due to dielectric saturation, defined here as the nonlinear response of $\langle\cos\theta\rangle$ at high fields, is given by

$$\Delta\phi_{sat} = N_q\mu(\langle\cos\theta_e\rangle_q - \langle\cos\theta\rangle_q)/R_q^2 \quad \text{(A4)}$$

where $\langle\cos\theta_e\rangle_q$ is the expected value of the mean dipole orientation at charge q. We define the expected value of the dipole orientation by noting from the dashed line in Figure 7 that for first-shell waters, $\langle\cos\theta\rangle$ varies/linearly with the magnitude of the radial field in the range $q = 0.25$ to $q = 0.75$. $\langle\cos\theta_e\rangle_q$ is then obtained by assuming that at the approximate midpoint of this range ($q = 0.5$) the response is linear and then carrying out a linear extrapolation of the field to higher values q. The mean radial field experienced by the dipoles varies as $1/R_q^2$. Thus

$$\langle\cos\theta_e\rangle = (q/0.5)(R_{0.5}^2/R_q^2)\langle\cos\theta\rangle_{0.5} \quad \text{(A5)}$$

Appendix B: Derivation of the Two-Shell Dielectric Model for a Spherical Ion

Consider a spherical ion of radius a and charge q surrounded by solvent. The solvent is considered to consist of two spherical shells, the first extending from the surface of the ion to a radius b, the second extending from b to infinity. The outer shell of solvent is assumed to behave with a constant dielectric of ϵ, while the inner shell has a dielectric of ϵ, up to a charge of q^*, and then abruptly saturates with a dielectric constant of ϵ_1. We require expressions for the electrostatic solvation energy, or the energy of transferring this ion from vacuum to the solvent, and for the reaction potential experienced by the ion. To obtain these expressions, it is convenient to assume that the charge of the ion is distributed uniformly over its surface, with density $\sigma = q/(4\pi a^2)$.

We start by writing the general solution to the Poisson equation for spherically symmetric systems for each of the two shells, assuming a constant dielectric of ϵ_1 for the inner shell, to obtain the potential, $\phi(r)$, where r is the radial coordinate, origin at the center of the ion:

inner shell: $$\phi_1 = A_1/\epsilon_1 r + B_1 \quad \text{(B1)}$$

outer shell: $$\phi_2 = A_2/\epsilon r + B_2 \quad \text{(B2)}$$

where the integration constants A_1, A_2, B_1, and B_2 are determined from the boundary conditions

$$\phi_1(b) = \phi_2(b) \quad \text{(B3)}$$

$$\epsilon_1\phi'_1(b) = \epsilon\phi'_2(b) \quad \text{(B4)}$$

$$\phi_2(\infty) = 0 \quad \text{(B5)}$$

$$\phi'_1(a) = -4\pi\sigma/\epsilon_1 \quad \text{(B6)}$$

The prime indicates the derivative with respect to r. Equations B1–B6 give

$$\phi_1 = q/\epsilon_1 r + q(1/\epsilon - 1/\epsilon_1)/b \quad \text{(B7)}$$

$$\phi_2 = q/\epsilon r \quad \text{(B8)}$$

The potential at the ion is

$$\phi(a) = q/\epsilon_1 a + q(1/\epsilon - 1/\epsilon_1)/b \quad \text{(B9)}$$

The potential at the ion in a vacuum is

$$\phi_v(a) = q/a \quad \text{(B10)}$$

and the reaction potential due to the solvent at the ion, $\Delta\phi_x$, is

$$\Delta\phi_x = q/\epsilon_1 a + q(1/\epsilon - 1/\epsilon_1)/b - q/a \quad \text{(B11)}$$

or

$$\Delta\phi_x = q(1/a - 1/b)(1/\epsilon_1 - 1) + q(1/\epsilon - 1)/b \quad \text{(B12)}$$

where the first and second terms of (B12) are the contributions to the reaction potential from the inner and outer dielectric shells, respectively. Now we must account for the fact that the dielectric of the first shell is not constant but has a value ϵ for $q < q^*$ and ϵ_1 for $q > q^*$. The change in reaction potential with charge is

$$\partial\Delta\phi_x/\partial q =$$

$$(1/a - 1/b)(1/\epsilon - 1) + (1/\epsilon - 1)/b \quad \text{for } q < q^* \quad \text{(B13)}$$

$$(1/a - 1/b)(1/\epsilon_1 - 1) + (1/\epsilon - 1)/b \quad \text{for } q > q^* \quad \text{(B14)}$$

Integrating to obtain the reaction potential at any q

$$\Delta\phi_x(q) = \int \delta q\, \partial\Delta\phi/\partial q \quad \text{(B15)}$$

$$\Delta\phi_x = q(1/\epsilon - 1)/a \quad \text{for } q \le q^* \quad \text{(B16)}$$

$$\Delta\phi_x = \Delta\phi_x(q^*) + (q - q^*)\,\partial\Delta\phi_x(q)/\partial q \quad \text{for } q > q^*$$

$$= q^*(1/\epsilon - 1)/a + (q - q^*)\{(1/a - 1/b)(1/\epsilon_1 - 1) + (1/\epsilon - 1)/b\} \quad \text{(B17)}$$

Combining terms of (B17) in the constant factor, q^*, gives

$$\Delta\phi_x = q\{(1/q - 1/b)(1/\epsilon_1 - 1) + (1/\epsilon - 1)/b\}\ \text{(slope)} + q^*\{(1/a - 1/b)(1/\epsilon - 1/\epsilon_1)\}\ \text{(intercept)} \quad \text{(B18)}$$

The solvation energy is given by

$$\Delta A = \int \Delta\phi_x\, dq \qquad dq = [0...q] \quad \text{(B19)}$$

Substituting for $\Delta\phi_x$ with eq B16–B17, integrating, and rearranging yield

$$\Delta A = q^*2(1/\epsilon - 1)/2a + q^*(q - q^*)(1/a - 1/b)(1/\epsilon - 1) + (q - q^*)^2(1/a - 1/b)(1/\epsilon_1 - 1)/2 + (q^2 - q^{*2})(1/\epsilon - 1)/2b \quad \text{(B20)}$$

If the substitution $q^* = q$ is made in eq B17 and B20, the familiar Born model is recovered (eq 1 and 5a of the text), while if $\epsilon_1 = 2$, $q^* = 0$, the model of Beveridge and Schnuelle[12] is obtained.